Domain organization and flavin adenine dinucleotide-binding determinants in the aerotaxis signal transducer Aer of *Escherichia coli*

Sergei I. Bibikov, Lindsey A. Barnes*, Yakov Gitin*, and John S. Parkinson†

Department of Biology, University of Utah, Salt Lake City, UT 84112

Communicated by Julius Adler, University of Wisconsin, Madison, WI, March 16, 2000 (received for review December 30, 1999)

Aerotactic responses in *Escherichia coli* are mediated by the membrane transducer Aer, a recently identified member of the superfamily of PAS domain proteins, which includes sensors of light, oxygen, and redox state. Initial studies of Aer suggested that it might use a flavin adenine dinucleotide (FAD) prosthetic group to monitor cellular redox changes. To test this idea, we purified lauryl maltoside-solubilized Aer protein by His-tag affinity chromatography and showed by high performance liquid chromatography, mass spectrometry, and absorbance spectroscopy that it bound FAD noncovalently. Polypeptide fragments spanning the N-terminal 290 residues of Aer, which contains the PAS motif, were able to bind FAD. Fusion of this portion of Aer to the flagellar signaling domain of Tsr, the serine chemoreceptor, yielded a functional aerotaxis transducer, demonstrating that the FAD-binding portion of Aer is sufficient for aerosensing. Aerotaxis-defective missense mutants identified two regions, in addition to the PAS domain, that play roles in FAD binding. Those regions flank a central hydrophobic segment needed to anchor Aer to the cytoplasmic membrane. They might contact the FAD ligand directly or stabilize the FAD-binding pocket. However, their lack of sequence conservation in Aer homologs of other bacteria suggests that they play less direct roles in FAD binding. One or both regions probably also play important roles in transmitting stimulus-induced conformational changes to the C-terminal flagellar signaling domain to trigger aerotactic behavioral responses.

redox sensing | prosthetic group | PAS domain | membrane topology

Motile bacteria exhibit many adaptive locomotor behaviors, the best studied of which is chemotaxis in *Escherichia coli* (see refs. 1–3 for recent reviews). These organisms use transmembrane chemoreceptors, known as methyl-accepting chemotaxis proteins (MCPs), to monitor and respond to changes in their chemical environment as they swim about. MCPs have a periplasmic ligand-binding domain that communicates via membrane-spanning segments with a cytoplasmic signaling domain, which forms stable complexes with the CheA and CheW proteins to transmit sensory information to the flagellar motors. Changes in receptor occupancy modulate conformation of the MCP signaling domain, thereby controlling the CheA histidine kinase, whose protein phosphorylation activity regulates the direction of motor rotation. MCPs are excellent models for exploring the molecular mechanisms of transmembrane signaling and sensory adaptation, but, despite extensive study, there are still significant gaps in our understanding of these important processes.

The recently discovered Aer protein is an MCP-like transducer that mediates aerotactic (oxygen-seeking) behavior in *E. coli* (4, 5). The sequence features of Aer suggest that it has an unorthodox domain organization and membrane topology whose study may shed light on the signaling mechanisms in more conventional MCPs (Fig. 1). The N terminus of Aer resembles a segment of NifL, an O_2-responsive regulatory protein that employs a bound flavin adenine dinucleotide (FAD) molecule as a redox sensor (6, 7).

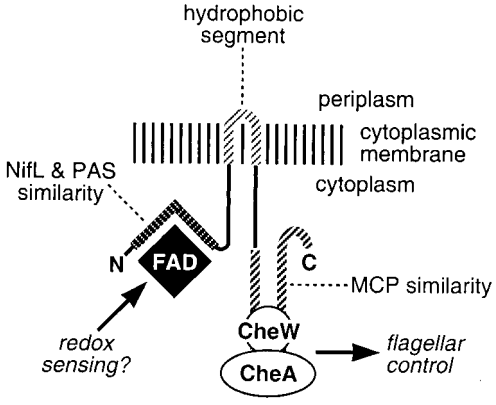

Fig. 1. Sequence features and working model of Aer.

Initial work on Aer suggested that it also bound FAD (4), presumably for sensing aerotactic stimuli in the form of cellular redox changes (8, 9). The N termini of Aer and NifL were subsequently shown to contain a PAS motif (10, 11), which in some proteins is known to comprise a binding pocket for a prosthetic group (reviewed in ref. 12). The putative NifL/PAS aerosensing domain of Aer is followed by a block of predominantly hydrophobic amino acids that may serve to anchor the protein to the cytoplasmic side of the inner membrane (4). The C terminus of Aer has high similarity to the signaling domains of MCPs (4, 5) and may form ternary complexes with CheA and CheW to control the cell's flagellar motors in response to aerotactic stimuli.

Here we report initial biochemical and genetic studies of Aer that examine key predictions of this working model. We show that Aer binds FAD noncovalently and that the N-terminal 290 residues of the protein are sufficient for this activity. Fusion of the FAD-binding portion of Aer to the flagellar signaling domain of Tsr, the serine chemoreceptor, yielded a functional aerotaxis transducer, demonstrating that the FAD-binding portion of Aer is sufficient for detecting aerotactic stimuli. We also describe a colony morphology assay for aerotaxis and its use in isolating non-aerotactic point mutants. We found aerotaxis-

Abbreviations: FAD, flavin adenine dinucleotide; MCP, methyl-accepting chemotaxis protein.

*Present address: School of Medicine, University of Utah, Salt Lake City, UT 84132.

†To whom reprint requests should be addressed. E-mail: Parkinson@Biology.Utah.edu.

The publication costs of this article were defrayed in part by page charge payment. This article must therefore be hereby marked "*advertisement*" in accordance with 18 U.S.C. §1734 solely to indicate this fact.

Article published online before print: *Proc. Natl. Acad. Sci. USA*, 10.1073/pnas.100118697. Article and publication date are at www.pnas.org/cgi/doi/10.1073/pnas.100118697

defective missense mutations throughout Aer. Those in the C-terminal signaling domain did not affect FAD binding whereas those in the N-terminal aerosensing domain did. The latter mutations fell mainly in the PAS motifs but also identified two other N-terminal regions that evidently play roles in FAD binding. Finally, we constructed deletions and point mutations in the central hydrophobic segment to test its postulated role as a membrane anchor. Proteins deleted for most of the hydrophobic segment failed to associate with the cytoplasmic membrane and could not support aerotactic ability. However, cysteine to alanine replacements at two positions in the hydrophobic segment had no deleterious effect on function, demonstrating that cysteine sulfhydryl chemistry is not involved in aerosensing by Aer.

Materials and Methods

Bacterial Strains. All bacterial strains used in this work were derivatives of *E. coli* K12. Isogenic derivatives of RP437, a wild-type reference strain for chemotaxis (13), included UU1117 [Δ*aer-1*] (4); RP3098 [Δ*(flhD-flhB)4*] (14); RP5700 [Δ*tsr-7028*] (15); and RP2361 [Δ*tar-3862*] (16). UU1259 [Δ*aer-1* Δ*tar-3862*] was constructed by introducing the *tar* mutation from RP2361 into UU1117 by phage P1-mediated cotransduction with the *eda* locus.

Plasmids. The parental plasmids used in this work were pCJ30, an isopropyl-β-D-thiogalactopyranoside-inducible p_{tac} expression vector (4), and pSB20, a pCJ30 derivative that expresses wild-type *aer* (4). Plasmid pSB50, which encodes a His-tagged version of the Aer protein, was constructed in two steps. First, a 1.5-kb *Pst*I-*Hin*dIII fragment containing the *aer* gene from pSB20 was cloned into pRSETc (Invitrogen), creating an in-frame fusion of the vector sequence encoding a 6xHis tag, AntiXpress epitope, enterokinase recognition sequence, and a short linker to the 5′ end of the *aer* coding region. Then, a 1.65-kb *Nde*I-*Hin*dIII fragment spanning the His-tagged *aer* gene was cloned into the *Nde*I-*Hin*dIII vector portion of pAR1, an isopropyl-β-D-thiogalactopyranoside-inducible expression plasmid similar to pCJ30 (17). The *Pst*I-*Hin*dIII segment in pSB50 was replaced with the corresponding segment from pSB20 *aer-D60N* to construct pSB51, which encodes a His-tagged version of the mutant Aer/D60N protein.

Plasmid pSB100, encoding a hybrid Aer-Tsr transducer, was constructed by high fidelity PCR synthesis of the 5′ portion of the *aer* coding region (codons 1–290) in pSB20 and the 3′ portion of the *tsr* coding region (codons 301–551) in pJC3, which carries the wild-type *tsr* gene (18). The *aer* fragment was treated with *Pst*I, the *tsr* fragment with *Hin*dIII, and pSB20 with both enzymes. The *aer* and *tsr* fragments were mixed with the vector portion of pSB20 and ligated. The resulting construct was confirmed by sequencing the entire *aer*/*tsr* coding region.

Aerotaxis Assay. Aerotactic ability was assessed on minimal semisolid agar medium (19) containing 30 mM sodium succinate as the principal carbon and energy source (4).

Isolation of Random Aer Point Mutants. Plasmid pSB20 was mutagenized by passage through RP526, a *mutD5* host (20), and was used to transform UU1117. Individual transformant colonies were screened for loss of aerotactic ability by toothpick transfer to succinate semisolid agar plates and were scored after overnight incubation at 35°C.

Construction of Site-Specific Aer Mutants. Cysteine codons 193, 203, and 253 in the *aer* gene of pSB20 were converted to alanine codons by high-fidelity PCR using mutation-bearing primers. The C193A C203A double was made by two successive rounds of mutagenesis. Double and triple mutant combinations with C253A were constructed by recombining the component mutations at a *Bgl*I restriction site that lies between codons 203 and 253. Aer truncation mutants were made by PCR synthesis of portions of the *aer* coding region that spanned a *Pst*I site at the 5′ end of the gene and ended at chosen 3′ positions within the coding region. The downstream primer introduced an in-frame stop codon and a *Hin*dIII restriction site. The resulting PCR products were treated with *Pst*I and *Hin*dIII and were cloned into the corresponding sites in pCJ30. Hydrophobic segment deletions were constructed by similar PCR methods, using oligonucleotide primers that introduced a short linker sequence and a *Bam*HI site in place of the hydrophobic segment. The upstream and downstream PCR fragments were joined at the *Bam*HI site and cloned into pCJ30, using the 5′ *Pst*I and 3′ *Hin*dIII sites. All site-specific *aer* mutations were verified by sequencing the entire mutant coding region.

Purification of Native Aer Proteins. Strain RP3098 containing plasmid pSB50 [*aer*$^+$] or pSB51 [*aer-D60N*] was grown at 37°C in H1 minimal medium (21) with 1% casamino acids, 0.4% glycerol, and 100 μg/ml ampicillin to early log phase. The cultures were induced with 1 mM isopropyl-β-D-thiogalactopyranoside and were grown for 4 h at 37°C. Cells from 2 liters of culture were collected by centrifugation, were frozen at −70°C, and then were resuspended in 30 ml of 50 mM Tris·HCl (pH 8.0), supplemented with DNase (30 units/ml), RNase (0.5 μg/ml), and protease inhibitors (200 μM phenylmethylsulfonyl fluoride, 2 μM leupeptin, and 1.5 μM pepstatin). The cells were broken by three passes through a French press at 10,000 psi and were centrifuged at 27,000 × *g* for 15 min to remove cell debris. Membranes were pelleted from the cell supernatant by centrifugation at 150,000 × *g* for 1 h and were resuspended in 5 volumes of 10 mM Tris·HCl (pH 8.0) and 40 mM KCl. Solid lauryl maltoside was added to a final concentration of 1%, and the membranes were stirred at 4°C for 15 min, then were centrifuged at 190,000 × *g* for 1 h to remove insoluble material. Imidazole was then added to the solubilized membranes to a final concentration of 10 mM, and the sample was applied to a Ni-NTA column (Qiagen, Chatsworth, CA). The column was washed with 10 mM imidazole in TKLM buffer (0.1% lauryl maltoside/10 mM Tris·HCl, pH 8.0/40 mM KCl) (22), followed by an additional wash with 20 mM imidazole in TKLM buffer. Aer protein was then eluted from the column with 100 mM imidazole in TKLM buffer.

Aer Overexpression Assay for FAD Binding. UU1117 carrying pSB20 derivatives with *aer* mutations was grown at 37°C to mid-log phase in 50 ml of H1 medium containing 1% casamino acids, 0.4% glycerol, and 100 μg/ml ampicillin. Aer synthesis was induced by addition of isopropyl-β-D-thiogalactopyranoside to a concentration of 1 mM, and the cells were grown for an additional 4 h, then collected by centrifugation at 6,000 × *g*. The cell pellet was resuspended in 1 ml of sterile water, and an equal volume of 6 M guanidine chloride was added to lyse the suspension. The sample was extracted several times with chloroform, discarding the organic phase. The remaining aqueous phase was further cleared with 0.22-μm low binding Durapore filters (Millipore), applied to a Microsorb C18 reverse phase column on a Waters 600 HPLC, and the FAD peak resolved as described earlier (4). The molecular weight of the peak material, determined by matrix-assisted laser desorption ionization time-of-flight mass spectrometry, also corresponded to that of FAD.

Identification of New Aer Homologs. Preliminary sequence data were obtained from The Institute for Genomic Research (TIGR) (http://www.tigr.org), the Sanger Centre (ftp://ftp.sanger.ac.uk/pub/pathogens/yp), and the Genome Sequencing Center (Washington University, St. Louis) (http://genome.wustl.edu/gsc/Projects/bacterial/salmonella.shtml). A BLAST (http://www.ncbi.nlm.nih.gov/BLAST/)search of partially sequenced bacterial genomes revealed putative Aer homologs in *Yersinia pestis* (Sanger Centre), *Vibrio cholerae* and *Shewanella putrefaciens* (TIGR Institute), and *Salmonella typhimurium* LT2 (Genome Sequence Center). Some of the proteins

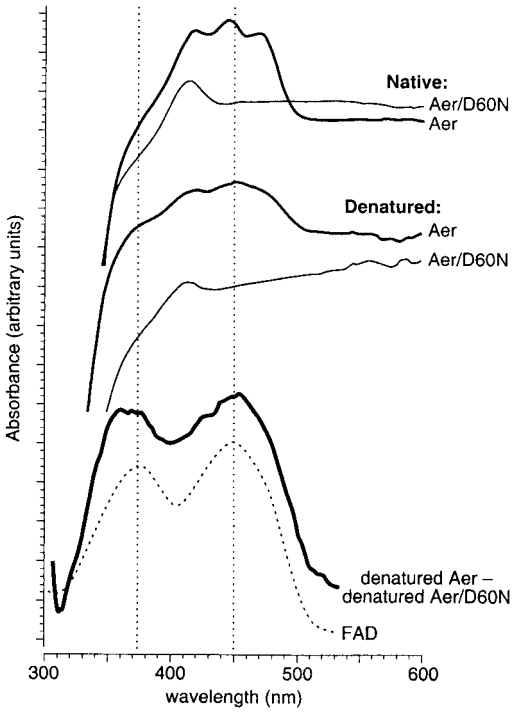

Fig. 2. Absorbance spectra of wild-type Aer and an FAD-binding mutant. His-tagged Aer proteins were solubilized in lauryl maltoside and were purified as detailed in *Materials and Methods*. Absorbance measurements were made with an Hitachi U-3300 UV/VIS spectrophotometer connected to a microcomputer. UV SOLUTIONS software (Hitachi Instruments, San Jose, CA) was used to obtain the differential spectrum shown at the bottom of the figure. The vertical dashed lines mark the two local absorbance maxima of FAD.

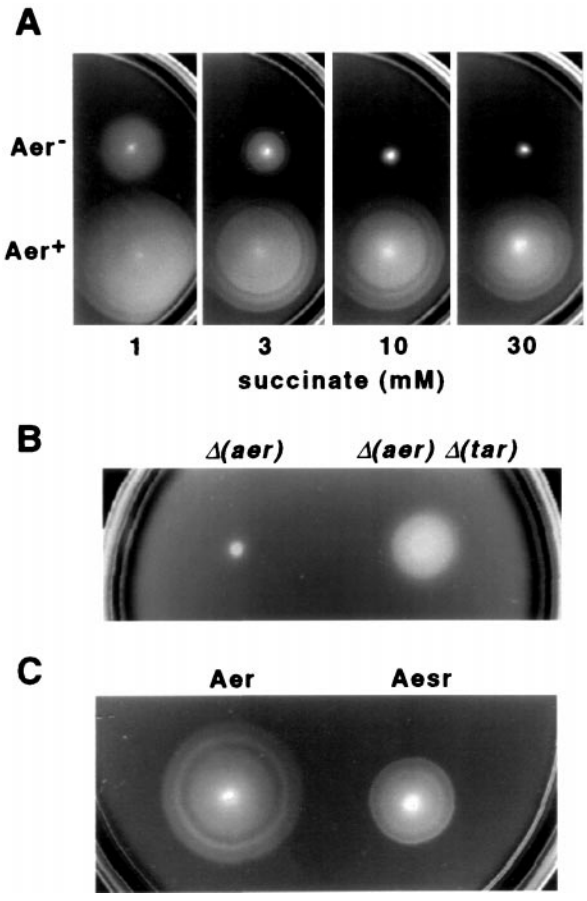

Fig. 3. Aerotaxis assays on succinate semisolid agar. Plates were photographed after incubation at 35°C for 18 h. (*A*) Colony morphology of Aer^- (UU1117) and Aer^+ (RP437) strains at different succinate concentrations. (*B*) Effect of Tar function on colony morphology of aerotaxis-defective strains, UU1117 [*Δ(aer) (tar⁺)*], and UU1259 [*Δ(aer) Δ(tar)*]. Plates contained 30 mM succinate. (*C*) Colony morphology of UU1117 containing pSB20 (Aer) or pSB100 (Aesr) at comparable levels of expression. Plates contained 30 mM succinate and 50 μg/ml ampicillin.

were manually assembled from contigs in the unfinished genomes. The primary structures of six newly found Aer homologs and two previously identified ones from *Pseudomonas putida* (23) and Tn*1721* (24) were aligned to *E. coli* Aer by the Clustal method (25) using DNASTAR software (DNAStar, Madison, WI.

Results

Association of FAD with Aer. In our initial study of Aer, we observed that cells expressing Aer at high levels also accumulated in their cytoplasmic membrane large amounts of FAD, which could be released into the aqueous fraction by treating the membranes with $CHCl_3$ (4). Accordingly, we proposed that Aer binds FAD noncovalently and that Aer overexpression stimulates concomitant overproduction of FAD within the cell. To exclude the possibility that overexpression of Aer only indirectly causes FAD accumulation in the membrane fraction, we have now constructed a His-tagged version of Aer and purified it from cell membranes solubilized in lauryl maltoside. Treatment of the purified material with guanidine hydrochloride, a protein denaturant, released two compounds whose masses coincided with a protonated form (molecular weight = 789) of FAD (molecular weight = 786) and its potassium salt (molecular weight = 827). We conclude that Aer binds FAD noncovalently, but apparently less avidly than typical flavoproteins, because its bound FAD was mostly released into the aqueous phase on overnight dialysis of the native protein (data not shown).

To validate the overexpression test for FAD binding by Aer, we compared the absorbance properties of His-tagged, solubilized, and purified wild-type Aer and a mutant protein (D60N, see below) with a putative FAD-binding defect based on the overexpression test (Fig. 2). The native wild-type protein exhibited three absorbance maxima at 420, 450, and 470 nm and a shoulder at 370–380 nm (Fig. 2, top). The mutant protein showed only the 420-nm peak (Fig. 2, top), which seemed to be associated with contaminating membrane cytochromes and gradually diminished on further purification (data not shown). Guanidine hydrochloride treatment of the wild-type protein eliminated the 470-nm peak, which we propose reflects the FAD-bound state of Aer (Fig. 2, middle). A difference spectrum of the denatured wild-type and mutant proteins revealed two absorbance peaks coincident with the long wavelength maxima for pure FAD (Fig. 2, bottom). These results demonstrate that Aer/D60N is defective in binding FAD. We propose that this binding defect is responsible for the inability of the D60N protein to induce elevated cellular levels of FAD and that the overexpression test can provide a qualitative assessment of FAD-binding ability in other mutant Aer proteins.

Isolation of Aerotaxis-Defective Mutants. Aer mutants were isolated from plasmid pSB20, which carries a wild-type *aer* gene expressed from a regulatable promoter (4). The plasmid was subjected to random mutagenesis, transferred into a *Δ(aer)* recipient strain, and the resultant colonies were screened for aerotactic ability on semisolid agar plates containing succinate as sole carbon and energy source (4). The respiratory activity of cells growing on succinate depletes the local oxygen supply and creates an oxygen gradient leading outward from the colony. Aerotactic colonies expand in pursuit of the oxygen remaining in the medium, aero-

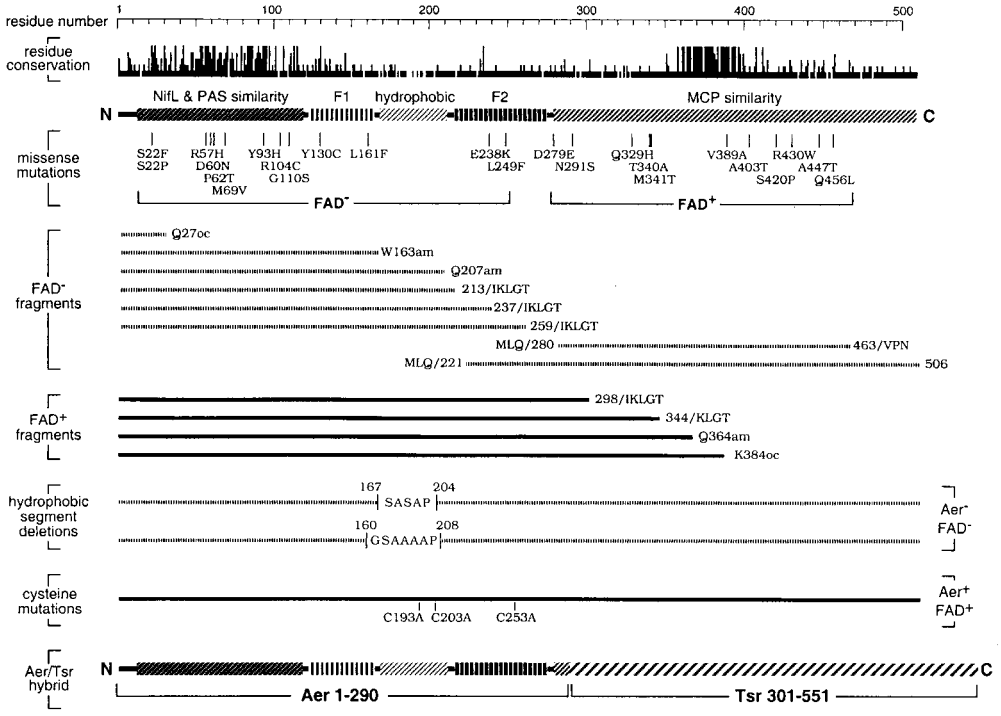

Fig. 4. FAD-binding properties of Aer missense mutants, deletions, and fragments. Residue conservation: The primary structures of Aer homologs from *P. putida*, Tn*1721*, *Y. pestis*, *V. cholerae* (three ORFs), *S. putrefaciens*, and *S. typhimurium* were aligned with that of *E. coli*. At each residue position, the height of the bar reflects the number of homologs with an amino acid identical to that of *E. coli* Aer. Missense mutations: The indicated amino acid replacements were found among *mutD*-induced, aerotaxis-defective mutants of pSB20. FAD binding by the mutant proteins was assessed by the overexpression test. FAD^-/FAD^+ fragments: The shaded and solid lines indicate the segment of the Aer protein made in nonsense mutants [oc, ochre (UAA); am, amber (UAG)] or from subcloned portions of the *aer* coding region. Capital letters at the ends of the fragments indicate vector-encoded amino acids; numbers indicate initial and final codons from *aer*. Hydrophobic segment deletions: Numbers give the *aer* codons at either end of the deletion; letters within the deletion gaps indicate amino acids of the joining linker. Neither deletion protein binds FAD or supports aerotaxis. Cysteine mutations: The positions of the three cysteine residues in Aer and their replacement mutations are shown. The triply mutant protein binds FAD and supports aerotaxis. Aer/Tsr hybrid: Domain schematic of the Aesr transducer, which has the signaling domain of Tsr and supports aerotaxis (see Fig. 3*C*).

taxis-defective colonies do not (Fig. 3*A*). At succinate concentrations of 10 mM or more, the difference in colony size is especially dramatic because aerotaxis-defective mutants remain at the site of inoculation, failing to spread even by random motility (Fig. 3*A*). This agoraphobic effect most likely arises from the ability of cells growing on succinate to produce and excrete aspartate, a powerful attractant for *E. coli* (26). Thus, aerotaxis-defective strains that also lacked the aspartate chemoreceptor formed considerably larger colonies at high succinate concentrations (Fig. 3*B*), suggesting that chemotaxis toward the aspartate released by the growing colony opposes outward diffusion of aerotaxis-defective cells. Evidently, the aerotactic response of wild-type cells overcomes the aspartate effect, enabling them to form a large colony with characteristic bands of cells congregated at the leading edge of the oxygen gradient. Although the serine chemoreceptor, Tsr, has also been implicated in aerotactic behavior (5), Tsr function did not influence the size or appearance of Aer^+ or Aer^- colonies on succinate plates, suggesting that Aer is the principal transducer for aerotaxis under these conditions (data not shown).

FAD-Binding by Aer Missense Mutants. After initial phenotype characterizations, protein expression tests, and DNA sequence analyses, 28 aerotaxis mutants of independent origin were analyzed for FAD-binding by the Aer overexpression test (Fig. 4). Among 24 mutants with single missense mutations, 11 fell in the region of MCP similarity, and all of those mutant proteins bound FAD by the overexpression test, consistent with the proposed output signaling function for this region of Aer. The remaining 13 missense mutants all expressed an Aer protein of wild-type size and stability (data not shown), but those proteins failed to bind FAD in the overexpression test. Nine of those mutations fell in the region of NifL/PAS similarity, consistent with its proposed role in forming the FAD-binding pocket. However, the other four FAD^- mutations were outside the originally noted Aer structural features: two fell between the NifL/PAS similarity and the hydrophobic segment, a region we designate "F1"; and two fell between the hydrophobic segment and the MCP similarity, a region we designate "F2."

The Aer proteins with amino acid replacements in regions F1 or F2 were each tested multiple times for ability to bind FAD by the overexpression test. The mutant proteins could be expressed at high levels and were associated with the cytoplasmic membrane, but they consistently failed to cause increased levels of FAD in the membrane fraction (data not shown). We conclude that regions F1 and F2 of Aer play a role in its ability to bind FAD.

FAD-Binding by Aer Fragments. Five of our aerotaxis-defective mutants had nonsense mutations that truncated the Aer protein at various positions. Aer fragments truncated at residue 27, 163, or 207 did not bind FAD whereas Aer fragments truncated at residue 364 or 384 did bind FAD (Fig. 4). Thus, Aer fragments containing the NifL/PAS segment were not able to bind FAD in the overexpression assay unless they also carried the F1, hydrophobic, and F2 segments. To more precisely delineate the FAD-binding portion of Aer, we constructed and examined some additional Aer fragments (Fig. 4). Aer (1–259) failed to bind FAD whereas Aer (1–298) did bind FAD. Thus, most or all

of the F2 segment is required for FAD binding, at least by Aer fragments starting at the N terminus.

The Hydrophobic Segment. To test whether the hydrophobic segment of Aer, spanning residues 168–209, was important for membrane anchoring, we constructed two mutants in which most of the hydrophobic residues were replaced with short, alanine-rich linkers (Fig. 4) and examined the cellular location of the deleted Aer proteins. Unlike wild-type Aer, the deleted proteins [AerΔ (168–203)/SASAP and AerΔ (161–207)/GSAAAAAP] failed to associate with the cytoplasmic membrane and, instead, accumulated in the soluble cell fraction (data not shown). Neither of the deleted proteins supported aerotactic ability (data not shown). High level expression of the proteins did not cause a concomitant elevation in the cellular content of FAD (data not shown), suggesting that membrane insertion might play a role in FAD binding. Alternatively, deletion of the hydrophobic segment might have disrupted the proper orientation of the flanking F1 and F2 segments, which in turn influence FAD binding.

None of our aerotaxis-defective missense mutants had alterations in the hydrophobic segment, suggesting that membrane insertion and any other functions of the hydrophobic segment are relatively insensitive to single amino acid changes. However, the hydrophobic segment does contain two cysteine residues (Cys-193 and Cys-203), which are otherwise quite rare in *E. coli* chemoreceptors of the MCP family. Moreover, Aer contains a third cysteine (Cys-253) in the F2 region. Cysteine's unique sulfhydryl chemistry is known to play a role in the redox-sensing abilities of other proteins (27), so even though these cysteines were not conserved in other Aer homologs, we wanted to directly test the possibility that they might play an important functional role in Aer. Accordingly, we constructed alanine-replacement mutations at each of the cysteine positions and tested their effects on Aer function. The three single replacement mutants, as well as double and triple mutant combinations, still supported normal aerotactic ability on succinate plates (data not shown), demonstrating that none of the three cysteine residues in Aer is necessary for aerosensing.

A Chimeric Aerosensor. Our point mutation and fragment analyses indicated that Aer residues 1–298 were sufficient for FAD-binding. To test whether this FAD-binding portion of Aer serves as an aerosensing input domain, we constructed a hybrid transducer in which residues 1–290 from Aer were fused to the signaling domain of Tsr (Fig. 4). The chimeric "Aesr" transducer mediated aerotaxis on succinate semisolid agar, although less effectively than did Aer at comparable expression levels (Fig. 3*C*). This result demonstrates that the N-terminal 290 residues of Aer are sufficient to detect aerotactic stimuli whereas its C-terminal 216 residues perform an output signaling function common to other MCP family chemoreceptors.

Discussion

The results presented in this report are consistent with the working model of Aer domain organization and membrane topology summarized in Fig. 1. The Aesr chimeric transducer demonstrates that the N-terminal portion of Aer detects aerotactic stimuli whereas its C-terminal portion is functionally homologous to the flagellar signaling domains in other bacterial chemoreceptors. Repik *et al.* (28) reached a similar conclusion with a slightly different Aesr construct.

The signaling domains of MCP molecules are deployed on the cytoplasmic side of the inner membrane, where they interact with the cytoplasmic CheW and CheA signaling proteins. Presumably, the corresponding portion of the Aer molecule is also located in the cytoplasmic compartment. The membrane topology of the aerosensing portion of Aer is less certain, but two lines of circumstantial evidence suggest that the N terminus of the Aer molecule is also located on the cytoplasmic side of the inner membrane. First, as discussed more extensively below, the aerosensing portion of Aer binds cellular FAD, which is synthesized in the cytoplasmic compartment. Second, Aer molecules with deletions of the central hydrophobic segment failed to associate with the cytoplasmic membrane, suggesting that the hydrophobic segment serves as a membrane anchor and is the principal topological determinant in the Aer molecule. The hydrophobic segment is long enough to traverse the membrane bilayer twice and, in fact, contains a proline residue at its midpoint that might facilitate the structural turn pictured in the working model. Thus, regions of the Aer molecule that adjoin both the N and C ends of the hydrophobic segment are most likely located on the cytoplasmic side of the membrane.

Aer binds FAD noncovalently, but apparently less avidly than typical flavoproteins, whose affinities for FAD or FMN fall in the submicromolar range (27). Several lines of evidence indicate that FAD-binding by Aer is mechanistically related to its ability to detect aerotactic stimuli. First, all critical FAD-binding determinants reside in residues 1–298, which corresponds to the aerosensing portion of the molecule. Second, all aerotaxis-defective missense mutations obtained in this portion of Aer also eliminated FAD-binding ability. Aer may detect aerotactic stimuli by using FAD to monitor cellular redox state [see review (9)]. On the one hand, bound FAD might function as a prosthetic group to trigger signaling conformational changes on oxidation or reduction. On the other hand, Aer might function as a conventional chemosensor by binding FAD reversibly, with differential affinity for its oxidized and reduced forms. In either model, Aer would detect cellular redox changes via FAD and in turn convey that information to its signaling domain to modulate locomotor behavior. The distribution of FAD-binding determinants in Aer provides important clues to the possible mechanisms of this input-output communication.

Aer's primary FAD-binding determinants most likely reside in its PAS domain (28). Recent reports suggest that the PAS motif specifies a small molecule binding pocket that can be adapted to fit a variety of ligands, including FAD [NifL (6) and Aer], but also FMN [NPH-1 (29)], heme [FixL (30)], 4-hydroxycinnamic acid [PYP (31)], and dioxin [ARH (32)]. X-ray structures of three PAS domains [PYP (33), FixL (34), and HERG (35)] reveal a common architecture consisting of a mixed α/β PAS core, an α-helical connector, and a β scaffold, altogether about 100 residues in length. We obtained aerotaxis-defective missense mutations in each of these three predicted structural features of Aer: Ser-22 (PAS core); Arg-57, Asp-60, Pro-62, and Met-69 (elements of the loop and helical connector between the PAS core and the β-scaffold); and Tyr-93, Arg-104, and Gly-110 (β-scaffold). Four of these residues are present in all Aer and NifL proteins and could conceivably make either direct, e.g., hydrogen-bonding, contacts to FAD (Ser-22, Met-69, and Tyr-93) or provide critical control of their relative orientation (Pro-62). None of these or the other PAS domain residues identified with aerotaxis- and FAD-binding defective mutations is conserved in NPH-1, an FMN-binding protein in *Arabidopsis*, although some have chemical characteristics in common (36).

We also found missense mutations outside the PAS domain that affected FAD-binding by Aer. Region F1 adjoins the N-end, and region F2 the C-end, of the hydrophobic segment. Both regions could contain residues that interact directly with the FAD ligand (Fig. 5*A*), but this seems unlikely because neither region bears significant similarity to the corresponding segments of eight Aer homologs in other bacteria (Fig. 4, residue conservation). Only a few F1 and F2 residues are highly conserved, and only one of our mutations in these regions fell at a conserved position (Y130). The lack of primary structure conservation suggests that F1 and F2 could play a less direct role in FAD binding. Those regions might stabilize the FAD-binding pocket through interactions with structural elements of the pocket (Fig. 5*B*), but such a role is also hard

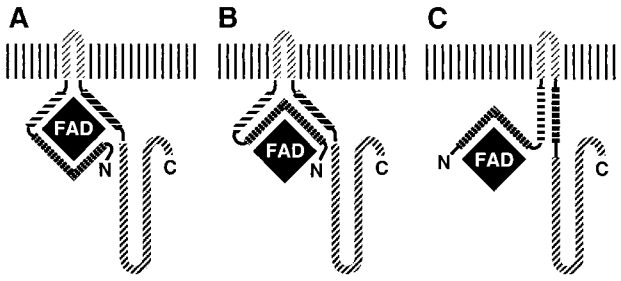

Fig. 5. Possible roles of the F1 and F2 segments of Aer. The shading conventions are the same ones used in Figs. 1 and 4: ▨, NifL/PAS similarity segment; IIII, F1 region; ▨, hydrophobic segment; **IIII**, F2 region; ▨, MCP similarity segment. (*A*) F1 and F2 directly comprise the FAD-binding pocket. (*B*) F1 and F2 stabilize the FAD-binding pocket through interactions with the NifL/PAS domain. (*C*) F1 and F2 indirectly stabilize the FAD-binding pocket. In all three models, input stimuli sensed by the FAD ligand, ostensibly via redox changes, are transmitted to the output signaling domain through the F2 region. The hydrophobic segment anchors Aer to the inner membrane, but otherwise may play no role in input-output communication.

to reconcile with the lack of sequence conservation in F1 and F2, because the NifL/PAS segment is highly conserved across the Aer homologs (Fig. 4). Alternatively, F1 and F2 might stabilize the FAD-binding pocket indirectly, through interactions that influence the folding pattern or overall structure, e.g., dimerization, of Aer. Conceivably, the F1 and F2 segments might interact with one another to stabilize the orientation of the FAD-binding pocket relative to other parts of the Aer molecule (Fig. 5*C*). Or, like other MCPs, Aer might function as a homodimer, and the F1 and F2 segments might play a role in dimerization.

The F2 region of Aer corresponds to a newly identified domain ["HAMP" (37); previously "linker" (38)] present in orthodox MCP chemoreceptors and some receptor histidine kinases. The HAMP domain or linker typically connects a transmembrane segment originating from a periplasmic sensing domain to a cytoplasmic signaling domain. These segments appear to play a crucial role in transmitting stimulus information from the sensing to the signaling domain. They are predicted to be α-helical, possibly coiled-coils, that act as conformational switches to modulate the activity of an adjoining signaling domain. The nature of the stimulus-induced motion that is propagated to them through the membrane-spanning segment remains a hotly debated topic, but the unusual membrane topology of Aer suggests that its HAMP domain/linker (F2) may respond to signals propagated directly through interaction with another cytoplasmic portion of the molecule, for example, the FAD ligand itself (Fig. 5*A*), the FAD-binding pocket (Fig. 5*B*), or the F1 segment (Fig. 5*C*). The existence of F2 mutations that disrupt FAD binding provides evidence of conformational coupling between the FAD-binding pocket and the region that most likely regulates output signaling activity in Aer.

All three of the signaling arrangements pictured in Fig. 5 predict that the hydrophobic segment may not be essential to Aer function, and, in fact, except for their predominantly hydrophobic character, the residues of the membrane anchor are not conserved in other Aer homologs. In particular, the two cysteine residues present in the hydrophobic segment of *E. coli* Aer, and a third in the F2/HAMP/linker segment, do not occur in other Aer proteins and are not essential for function. Nevertheless, the two hydrophobic segment deletions we constructed proved defective in FAD-binding and aerotaxis. These particular deletions may have simply disrupted the proper interaction of F2 with its partner, but perhaps membrane insertion *per se* is important for Aer function. Conceivably, membrane association enables Aer to detect aerotactic stimuli: for example, via redox changes in a component of the electron transport chain. Further genetic studies of Aer, using the kinds of tools described in this report, should help to resolve this issue.

The authors thank Barry Taylor, Mark Johnson, and Igor Zhulin for helpful comments on this manuscript and the following for communication of DNA sequence data before publication: Carrie Harwood (University of Iowa), The Genome Sequencing Center (Washington University, St. Louis), the *Yersinia pestis* Sequencing Group at the Sanger Centre; and The Institute for Genomic Research. This work was supported by Research Grant 5-R37-GM19559 from the National Institutes of Health and by the University of Utah Research Foundation Funding Incentive Seed Grant Program. The Protein-DNA Core Facility and the Mass Spectrometry Facility at the University of Utah receive support from National Cancer Institute Grant CA42014 to the Huntsman Cancer Institute. L.A.B and Y.G. received support from the Bioscience Undergraduate Research Program, Department of Biology, University of Utah.

1. Armitage, J. P. (1999) *Adv. Microbiol. Physiol.* **41,** 229–289.
2. Stock, J. B. & Surette, M. G. (1996) in *Escherichia coli and Salmonella: Cellular and Molecular Biology*, eds. Neidhardt, F. C., Curtiss, R., Ingraham, J. L., Lin, E. C. C., Low, K. B., Magasanik, B., Reznikoff, W. S., Riley, M., Schaechter, M. & Umbarger, H. E. (Am. Soc. Microbiol., Washington, DC), Vol. I, pp. 1103–1129.
3. Blair, D. F. (1995) *Annu. Rev. Microbiol.* **49,** 489–522.
4. Bibikov, S. I., Biran, R., Rudd, K. E. & Parkinson, J. S. (1997) *J. Bacteriol.* **179,** 4075–4079.
5. Rebbapragada, A., Johnson, M. S., Harding, G. P., Zuccarelli, A. J., Fletcher, H. M., Zhulin, I. B. & Taylor, B. L. (1997) *Proc. Natl. Acad. Sci. USA* **94,** 10541–10546.
6. Soderback, E., Reyes-Ramirez, F., Eydmann, T., Austin, S., Hill, S. & Dixon, R. (1998) *Mol. Microbiol.* **28,** 179–192.
7. Macheroux, P., Hill, S., Austin, S., Eydmann, T., Jones, T., Kim, S. O., Poole, R. & Dixon, R. (1998) *Biochem. J.* **332,** 413–419.
8. Bespalov, V. A., Zhulin, I. B. & Taylor, B. L. (1996) *Proc. Natl. Acad. Sci. USA* **93,** 10084–10089.
9. Taylor, B. L., Zhulin, I. B. & Johnson, M. S. (1999) *Annu. Rev. Microbiol.* **53,** 103–128.
10. Zhulin, I. B., Taylor, B. L. & Dixon, R. (1997) *Trends Biochem. Sci.* **22,** 331–333.
11. Ponting, C. P. & Aravind, L. (1997) *Curr. Biol.* **7,** R674–R677.
12. Taylor, B. L. & Zhulin, I. B. (1999) *Microbiol. Mol. Biol. Rev.* **63,** 479–506.
13. Parkinson, J. S. & Houts, S. E. (1982) *J. Bacteriol.* **151,** 106–113.
14. Smith, R. A. & Parkinson, J. S. (1980) *Proc. Natl. Acad. Sci. USA* **77,** 5370–5374.
15. Callahan, A. M., Frazier, B. L. & Parkinson, J. S. (1987) *J. Bacteriol.* **169,** 1246–1253.
16. Slocum, M. K. & Parkinson, J. S. (1983) *J. Bacteriol.* **155,** 565–577.
17. Wolfe, A. J. & Stewart, R. C. (1993) *Proc. Natl. Acad. Sci. USA* **90,** 1518–1522.
18. Chen, J. (1992) Ph. D. thesis (Univ. of Utah, Salt Lake City).
19. Ames, P. & Parkinson, J. S. (1988) *Cell* **55,** 817–826.
20. Cox, E. C. & Horner, D. L. (1983) *Proc. Natl. Acad. Sci. USA* **80,** 2295–2299.
21. Parkinson, J. S. (1976) *J. Bacteriol.* **126,** 758–770.
22. Mitchell, D. M. & Gennis, R. B. (1995) *FEBS Lett.* **368,** 148–150.
23. Nichols, N. N. & Harwood, C. S. (2000) *FEMS Microbiol. Lett.* **182,** 177–183.
24. Allmeier, H., Cresnar, B., Greck, M. & Schmitt, R. (1992) *Gene* **111,** 11–20.
25. Higgins, D. G. & Sharp, P. M. (1988) *Gene* **73,** 237–244.
26. Budrene, E. O. & Berg, H. C. (1995) *Nature (London)* **376,** 49–53.
27. Curti, B., Ronchi, S. & Zanetti, G. (1991) *Proceedings of the Tenth International Symposium on Flavins and Flavoproteins* (de Gruyter, Berlin).
28. Repik, A., Rebbapragada, A., Johnson, M. S., Haznedar, J. O., Zhulin, I. B. & Taylor, B. L. (2000) *Mol. Microbiol*., in press.
29. Christie, J. M., Reymond, P., Powell, G. K., Bernasconi, P., Raibekas, A. A., Liscum, E. & Briggs, W. R. (1998) *Science* **282,** 1698–1701.
30. Gilles-Gonzalez, M. A., Ditta, G. S. & Helinski, D. R. (1991) *Nature (London)* **350,** 170–172.
31. McRee, D. E., Tainer, J. A., Meyer, T. E., Van Beeumen, J., Cusanovich, M. A. & Getzoff, E. D. (1989) *Proc. Natl. Acad. Sci. USA* **86,** 6533–6537.
32. Whitelaw, M. L., Gottlicher, M., Gustafsson, J. A. & Poellinger, L. (1993) *EMBO J.* **12,** 4169–4179.
33. Borgstahl, G. E., Williams, D. R. & Getzoff, E. D. (1995) *Biochemistry* **34,** 6278–6287.
34. Gong, W., Hao, B., Mansy, S. S., Gonzalez, G., Gilles-Gonzalez, M. A. & Chan, M. K. (1998) *Proc. Natl. Acad. Sci. USA* **95,** 15177–15182.
35. Morais Cabral, J. H., Lee, A., Cohen, S. L., Chait, B. T., Li, M. & Mackinnon, R. (1998) *Cell* **95,** 649–655.
36. Huala, E., Oeller, P. W., Liscum, E., Han, I. S., Larsen, E. & Briggs, W. R. (1997) *Science* **278,** 2120–2123.
37. Aravind, L. & Ponting, C. P. (1999) *FEMS Microbiol. Lett.* **176,** 111–116.
38. Williams, S. B. & Stewart, V. (1999) *Mol. Microbiol.* **33,** 1093–1102.